High-mass X-ray Binaries: Illuminating the Passage from Massive Binaries to Merging Compact Objects
Proceedings IAU Symposium No. 346, 2019
L. M. Oskinova, E. Bozzo, T. Bulik & D. Gies, eds.

doi:10.1017/S1743921319001261

Numerical models of VHE emission by magnetic reconnection in X-ray binaries: GRMHD simulations and Monte Carlo cosmic-ray emission

J. C. Rodríguez-Ramírez, E. M. de Gouveia Dal Pino and R. Alves Batista

Instituto de Astronomia, Geofísica e Ciências Atmosféricas (IAG-USP), Universidade de São Paulo. Cidade Universitaria R. do Matão, 1226 05508-090 São Paulo, SP Brasil
email: juan.rodriguez@iag.usp.br

Abstract. Galactic microquasars have been detected at very-high-energies (VHE) (>100 GeV) and the particle acceleration mechanisms that produce this emission are not yet well-understood. Here we investigate a hadronic emission scenario where cosmic-rays (CRs) are accelerated in magnetic reconnection events by the turbulent, advected-dominated accretion flow (ADAF) believed to be present in the hard state of black hole binaries. We present Monte Carlo simulations of CR emission plus γ-γ and inverse Compton cascades, injecting CRs with a total energy consistent with the magnetic energy of the plasma. The background gas density, magnetic, and photon fields where CRs propagate and interact are modelled with general relativistic (GR), magneto-hydrodynamical simulations together with GR radiative transfer calculations. Our approach is applied to the microquasar Cygnus X-1, where we show a model configuration consistent with the VHE upper limits provided by MAGIC collaboration.

Keywords. radiation mechanisms: non-thermal, X-rays: binaries, magnetohydrodynamics, accretion disks

1. Introduction

Galactic microquasars are natural laboratories to study high energy emission processes having the advantage of being relatively close and undergoing processes in shorter time scales than high energy extragalactic sources like active galactic nuclei (AGNs) or quasars. Interestingly, there is no current unified model able to explain the very-high-energy (VHE) emission from these galactic sources: whether they have a hadronic and/or leptonic origin and if they are produced in outflows of pc scales and/or in compact regions.

The diverse nature of microquasrs' VHE emssion can be seen in the case of the sources SS 433 and Cygnus X-1. The VHE emission from SS 433 has recently been localised in outflows of pc scales launched by the binary system, with physical conditions that appear to favour a leptonic origin (Abeysekara *et al.* 2018). On the other hand, the multi-wavelength analysis on Cygnus X-1 by MAGIC Collaboration *et al.* (2017), ruled out any VHE emission correlated with the one-sided jet during the hard state (HS), suggesting that the VHE activity observed by MAGIC (Albert *et al.* 2007), might be produced inside the binary. Thus, improved observations as well as further development of theoretical models are required to clarify the origin of VHE emission from microquasars.

In this work, we investigate a hadronic emission scenario where CRs are accelerated by magnetic reconnection in a turbulent magnetised advection dominated accretion flow (ADAF) (see Singh *et al.* 2015; Kadowaki *et al.* 2015), thought to be present in the

HS of microquasars (Narayan & McClintock 2008; Yuan & Narayan 2014). Turbulent magnetic reconnection has been previously investigated with analytical and numerical approaches (de Gouveia Dal Pino & Lazarian 2005, de Gouveia Dal Pino *et al.* 2010, Kowal *et al.* 2011, 2012, Kadowaki, de Gouveia Dal Pino & Stone 2018, Kadowaki *et al.*, these proceedings) indicating that this mechanism could efficiently accelerate CRs in the surrounding of BH accretion flows (from microquasar to AGNs). This work is also motivated by previous hadronic emission models aimed to explain the VHE radiation from microquasars (Romero, Vieyro & Vila 2010; Vieyro & Romero 2012; Khiali de Gouveia Dal Pino & del Valle 2015).

The study presented here is based on Monte Carlo (MC) simulations of CRs that interact with a target environment obtained from GRMHD simulations together with GR radiative transfer calculations. With this approach we aim to provide a more self-consistent emission model with fewer free parameters in comparison with previous one-zone approaches (Khiali *et al.* 2015). In the next section we describe the numerical background model for the gas density, magnetic, and radiation field that we employ as the target for CRs interactions. In Section 3 we describe the Monte Carlo CR simulation applied to model the VHE emission of Cygnus X-1. Finally, we state our conclusions in Section 4.

2. The numerical ADAF background environment

If CRs are accelerated by magnetic reconnection in the turbulent accretion flow to the BH in the binary systems, they will mainly interact with the gas density, magnetic, and photon field of the accreting plasma, as well as with the radiation of the companion star. In the binary system Cygnus-X-1 the companion is inferred to be a O9.7 supergiant star (Orosz *et al.* 2011) and its radiation is expected to be important for VHE processes, specially around the superior conjunction of the compact object (Bosch-Ramon, Khangulyan & Aharonian 2008, Khiali *et al.* 2015). The present study is limited to consider only the radiation produced by the accretion flow; we will explore additional effects due to the stellar radiation field in a forthcoming work.

We adopt a GRMHD ADAF model and numerically obtain the gas density, magnetic, and photon fields employing the GRMHD axi-symmetric `harm` code (Gammie *et al.* 2003) together with the post-processing GR radiative transfer `grmonty` code (Dolence *et al.* 2009). In Fig. 1 we show the gas density, magnetic and photon fields of the snapshot that we set up as the environment where CRs propagate and interact.

These snapshot maps correspond to an accretion flow around a rotating BH of mass $M = 14.8\ \mathrm{M}_\odot$, with dimensionless spin parameter $a = 0.93$, at a evolution time $t = 2500 R_g/c$, being $R_g = GM/c^2 \simeq 2.2 \times 10^6$cm the gravitational radius. The plasma evolved from an initial equilibrium state where the accretion is triggered by magneto-rotational-instabiliy, similar to numerical GRMHD studies done by Mościbrodzka *et al.* (2009), O' Riordan *et al.* (2016) and others. The gas density is normalised to have a maximum value of $n = 5 \times 10^{17}\ \mathrm{cm}^{-3}$ and we use an ion-to-electron temperature of $T_p/T_e = 25$ to calculate the background photon field produced by synchrotron+IC scattering. The SED associated to this photon field is the cyan histogram plotted in Fig. 2 (left), assuming a distance to the binary of 1.8 kpc (Reid *et al.* 2011). We employ these numerical profiles for the background environment to simulate the propagation of CRs and their secondaries, as we describe in the next section.

3. Monte Carlo calculations of CR emission

We simulate the propagation and interactions of CRs employing the `CRPropa3` code (Alves Batista *et al.* 2016) where we inject CRs, all of them assumed to be protons,

https://doi.org/10.1017/S1743921319001261 Published online by Cambridge University Press

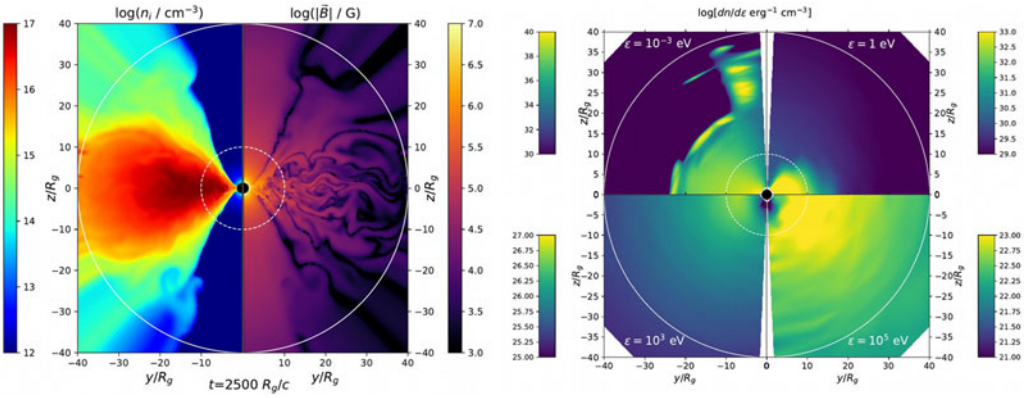

Figure 1. Left: gas density and magnetic field maps of the accretion flow environment where we simulate the propagation and interaction of CRs. This snapshot profiles are obtained with the GRMHD `harm` code. Right: photon field maps of synchrotron+IC radiation obtained by performing post-processing radiative transfer on the plasma snapshot on the left, employing the `grmonty` code. Each panel displays the photon field density for a fixed photon energy as indicated. The inner dashed circle represents the boundary within which we inject CRs assumed accelerated by magnetic reconnection. The outer solid circle represents the spherical boundary where we detect the radiation flux.

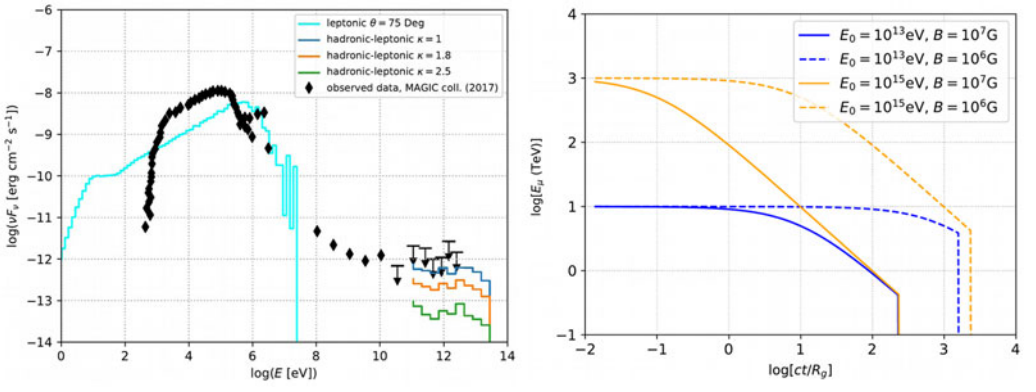

Figure 2. Left: SED of Cygnus X-1 corresponding to the hard state. The cyan histogram is the radiation flux obtained with leptonic synchrotron+IC employing the `grmonty` code (see Section 2). The histograms at energies > 100 GeV are γ-ray fluxes obtained from simulated hadronic interaction plus γ-γ and IC cascading employing the `CRPropa3` code (see Section 3). The data points and upper limits are taken from MAGIC Collaboration *et al.* (2017). Right: Estimation of muon synchrotron cooling. The curves represent energy of muons as a function of time (scale with the BH mass) in a uniform magnetic field, and with initial energy E_0 as indicated in the plot. The discontinuity in the curves indicates the time at which muons decay into neutrinos.

and accelerated by magnetic reconnection in the BH accretion flow of the binary. The 3D trajectories of charged particles (CRs and secondary leptons) are calculated by integrating the relativistic Lorentz force equation with the magnetic field of the GRMHD snapshot of Fig. 1. The gas density and photon field of the same snapshot are used to calculate the interactions rates for particles and photons along their trajectories, where these interactions are simulated with a Monte Carlo approach.

We then simulate (i) photo-pion processes, (ii) proton-proton interactions of CRs with thermal ions, (iii) γ-γ and IC cascading, and (iv) synchrotron cooling of charged particles. VHE γ-rays are produced out of photo-pion and proton-proton reactions and their

https://doi.org/10.1017/S1743921319001261 Published online by Cambridge University Press

attenuation is accounted by the γ-γ/IC cascades. We do not follow the photons produced by synchrotron cooling, nevertheless this process is employed to account for energy losses of charged particles (CRs and secondary leptons). We inject 10^4 isotropic CRs within a radius of $10R_g$ with energies in the range of 10^{14}-10^{16} eV, with a power-law energy distribution of index 1. Particles and photons are tracked until they complete a total trajectory of $150R_g$, or attain a minimum energy of 10^{11}eV, or else cross the spherical boundary at $40R_g$ (represented with the outer circle in Fig. 1).

The observed SED is calculated neglecting further emission and/or absorption of γ-rays beyond the detection boundary at 40 R_g from the BH (the radiation of the companion will be considered in a forthcoming work). Thus, the flux of radiation within the energy bin ϵ is given as

$$\nu F_\nu = (4\pi R_s^2)^{-1}\epsilon^2 \frac{N_\epsilon}{\Delta\epsilon \Delta t}(\text{erg s}^{-1}\text{cm}^{-2}), \tag{3.1}$$

where, $R_s = 1.8$ kpc is the distance to the binary system (Reid *et al.* 2011), Δt is the detection time interval, and N_ϵ is the number of detected physical photons within the energy bin ϵ.

The number of physical photons produced by CRs injected within the energy bin ϵ_0, which we label as $N_{\epsilon(\epsilon_0)}$, is calculated from the simulation output considering the condition $N_{\epsilon(\epsilon_0)}/N^{sim}_{\epsilon(\epsilon_0)} = N_{CR,\epsilon_0}/N^{sim}_{CR,\epsilon_0}$. The first term of this condition is the ratio of physical to simulated γ-rays within the energy bin ϵ and the second term is the ratio of physical to simulated CRs within the energy bin ϵ_0. Thus, the number of physical γ-rays as a function of the simulated γ-rays produced by CRs with initial energy ϵ_0 is calculated as

$$N_{\epsilon(\epsilon_0)} = \frac{A_\kappa \epsilon_0^{-\kappa}}{A_1 \epsilon_0^{-1}} N^{sim}_{\epsilon(\epsilon_0)} = \frac{E_{rec}}{N_{CR}} \frac{(2-\kappa)\ln(\epsilon_{max}/\epsilon_{min})}{\epsilon_{max}^{2-\kappa} - \epsilon_{min}^{2-\kappa}} \epsilon_0^{1-\kappa} N^{sim}_{\epsilon(\epsilon_0)}. \tag{3.2}$$

In the second term of the equations (3.2), A_κ is the normalisation constant of the power-law distribution of physical CRs with power-law index κ, and A_1 is the normalisation constant of the power-law distribution of simulated CRs with power-law index=1. The distribution of physical CRs is normalised with the total energy E_{rec} released by magnetic reconnection, and the distribution of simulated CRs with the total number of injected CRs, N_{CR}. In the third term of the equations (3.2), $\epsilon_{min} = 10^{14}$ eV and $\epsilon_{max} = 10^{16}$ eV are the maximum and minimum energy of injected CRs. In this manner, we weigh the simulation output, performed with a power-law index=1 of injected CRs, to obtain γ-ray fluxes corresponding to different power-law indices of CR injection.

In Fig. 2 we show the calculated emission flux that results from a simulation with $E_{rec} = 5 \times 10^{35}$ erg stored in CRs (which is consistent with magnetic reconnection energy released by an accretion plasma with $B \sim 10^7$ G within $10R_g$, according to the model by Singh, de Gouveia Dal Pino & Kadowaki 2015). The different histograms for $E > 11$ eV correspond to different power-law injection indices, as indicated.

Photo-pion and proton-proton reactions also produce neutrinos and electrons. However, due to the strong magnetic fields close to the BH of the binary, charged pions and muons are expected to cool down considerably before decaying into neutrinos and electrons. Here we do not report the neutrino fluxes associated to the simulated hadronic processes, as the propagation of pions and muons are not considered in the present calculation∗. Nevertheless, here we estimate muon cooling by synchrotron radiation (see Fig. 2, right) from which we expect that neutrinos that originated close to the BH would be detected

∗ Pions and muons are assumed to decay instantaneously in CRPropa3, as this code is originally aimed for cosmological propagation of CRs where the cooling of charged pions and muons is negligible.

https://doi.org/10.1017/S1743921319001261 Published online by Cambridge University Press

only below 10^{13} eV energies (see also the paper by Reynoso & Romero 2009, where this effect has been investigated in detail).

4. Summary and discussion

Here we investigate the VHE emission from the accretion flow of Cygnus X-1 with a numerical approach based on:

- a GRMHD ADAF plus GR radiative transfer simulated model of the accretion flow,
- particle acceleration by magnetic reconnection, and
- MC simulations of CRs plus γ-γ/IC cascading.

Assuming that CRs are efficiently accelerated by magnetic reconnection in the turbulent accretion flow (Kadowaki *et al.* these proceedings.), we simulate a burst-like injection of CRs (appropriate to study the flare nature of the VHE emission from Cygnus-X1) and obtain a radiation flux consistent with the VHE upper limits of Cygnus X-1. This VHE flux is obtained injecting CRs with a total energy of 5×10^{35} erg (consistent with the energy release by reconnection in an ADAF with $B \simeq$ of 10^7G inside a region of $10R_g$), within the energy range of 10^{14}-10^{16}eV.

Neutrinos fluxes are not calculated from our simulation, as propagation of pions and muons is required. However, we estimate that neutrino fluxes, if produced by reconnection close to the BH of Cygnus X1, would be detected with energies below 10^{13} eV.

We applied our method to Cygnus X-1 in this work, but this model can also be applicable to other microquasars displaying VHE emission, as well as to AGNs (Rodríguez-Ramírez *et al.* 2018). To obtain more consistent predictions, we intend include the companion's radiation in our models, together with pion and muon propagation to also obtain predictions for neutrino emission. The results of these implementations will be reported in a forthcoming paper.

Acknowledgments

We acknowledge support from the Brazilian agencies FAPESP (grant 2013/10559-5) and CNPq (grant 308643/2017-8). The simulations presented in this lecture have made use of the computing facilities of the GAPAE group (IAG-USP) and the Laboratory of Astroinformatics IAG/USP, NAT/Unicsul (FAPESP grant 2009/54006-4). RAB is supported by the FAPESP grant 2017/12828-4 and JCRR by the FAPESP grant 2017/12188-5.

References

Abeysekara, A. *et al.* 2018, *Nature*, 562, 82
Albert, J. *et al.* 2007, *ApJ*, 665, L51
Alves Batista, R., Dundovic, A., Erdmann, M., Kampert, K.-H., Kuempel, D., Mller, G., Sigl, G.; van Vliet, A., Walz, D., Winchen, T. 2016, *JCAP*, 05, 038A
Bosch-Ramon V., Khangulyan D., & Aharonian F. A. 2008, *A&A*, 489, L21
de Gouveia Dal Pino, E. M. & Lazarian, A. 2005, *A&A*, 441, 845,
de Gouveia Dal Pino, E. M., Piovezan, P. P., & Kadowaki, L. H. S. 2010, *A&A*, 518, A5
Dolence, J., Gammie, C., Mościbrodzka, M., & Leung, P-A. 2009, *ApJ*, 184, 387
Gammie, C., McKinney, J., & Toth, G. 2003, *ApJ*, 598, 444
Kadowaki, L. H. S., de Gouveia Dal Pino, E. M., & Singh, C. B. 2015, *ApJ*, 802, 113
Kadowaki, L. H. S., de Gouveia Dal Pino, E. M., & Stone, J. 2018, *ApJ*, 864, 52
Khiali, B., de Gouveia Dal Pino, E. M., & del Valle, M. V. 2015, *MNRAS*, 449, 34
Kowal G., de Gouveia Dal Pino E. M., & Lazarian, A. 2011, *ApJ*, 735, 102
Kowal G., de Gouveia Dal Pino E. M., & Lazarian, A. 2012, *PRL*, 108, 1102
MAGIC Collaboration 2017, *MNRAS*, 472, 3474

https://doi.org/10.1017/S1743921319001261 Published online by Cambridge University Press

Mościbrodzka, M., Gammie, C. F., Dolence, J. C., Shiokawa, H., & Leung, P. K. 2009, *ApJ*, 706, 497
Narayan, R., & McClintock, J. E. 2008, *NewAr*, 51, 733
O' Riordan, M., Pe'er, A. & McKinney, J. 2016, *ApJ*, 819, 95
Orosz J. A., McClintock J. E., Aufdenberg J. P., Remillard R. A., Reid M. J., Narayan R., & Gou L. 2011, *ApJ*, 742, 84
Reid M. J., McClintock J. E., Narayan R., Gou L., Remillard R. A., & Orosz J. A. 2011, *ApJ*, 742, 83
Reynoso, M. M., & Romero, G. E. 2009, *A&A*, 493, 1
Rodríguez-Ramírez, J. C., de Gouveia Dal Pino E. M., & Alves Batista, R. A. 2018, arXiv:1811.02812
Romero, G. E., Vieyro, F. L. & Vila, G. S. 2010, *A&A*, 519, 109
Singh C. B., de Gouveia Dal Pino E. M., & Kadowaki L. H. S. 2015, *ApJ*, 799, L20
Vieyro, F. L. & Romero G. E. 2012, *A&A*, 542, A7
Yuan, F. & Narayan, R. 2014, *ARA&A*, 52, 529

https://doi.org/10.1017/S1743921319001261 Published online by Cambridge University Press